Neuroradiology (1993) 35: 234–237

Neuro radiology

© Springer-Verlag 1993

MRI in craniofacial fibrous dysplasia

J. W. Casselman[1], I. De Jonge[2], L. Neyt[3], C. De Clercq[3], and G. D'Hont[4]

Departments of [1] Radiology, [2] Pathology, [3] Maxillofacial Surgery, [4] Otorhinolaryngology, St. Jan Hospital, Bruges, Belgium

Received: 10 October 1991

Summary. Five patients with biopsy-proven craniofacial fibrous dysplasia underwent MRI with T1- and T2-weighted sequences and a gadolinium-enhanced T1-weighted spin-echo sequence. Low to intermediate signal intensity was usually seen in the largest part of the lesion on both spin-echo sequences, but smaller regions of hyperintensity on T1- and T2-weighted images and intermediate signal intensity throughout a lesion on T1-weighted images were also seen. All lesions enhanced but only two became iso- or hyperintense compared to fat. High clinical and pathological activity in three cases correlated with high signal intensity on both spin-echo sequences and with strong enhancement in two of the three. The presence of large veins or sinusoids on pathological examination did not correlate with the enhancement pattern.

Key words: Bones, dysostoses – Fibrous dysplasia – Magnetic resonance imaging – Osteochondrodysplasias

Fibrous dysplasia (FD) is one of the most common benign skeletal disorders [1]. The skull and facial skeleton are involved in 25% of patients with the monostotic form and in 40–60% of those patients with the polyostotic form [2]. The typical plain film and CT changes are well known [3, 4]. There have been few reports on MRI [5–8] and even fewer on contrast-enhanced MRI [8, 9]. The likelihood of finding this relatively common skeletal disorder during a routine brain study is not small and so one should be familiar with the MRI patterns. We studied MRI signal characteristics on T1- and T2-weighted images in five patients with craniofacial FD, and the enhancement pattern following gadolinium-DOTA (Gd-DOTA), and looked for signal characteristics which could distinguish active and inactive lesions.

Patients and methods

Five females (average age 33 years, range 13–57 years) with biopsy-proven craniofacial FD underwent MRI. Three had monostotic disease, involving the mandible, maxilla or orbital roof and two had multiple foci: temporal bone and skull vault, sphenoid bone and lumbar vertebra. All patients were studied on a 1.0 T system. A standard quadrangular head coil was used and all patients underwent unenhanced T1-weighted (600/15/2 – TR/TE/excitations) and T2-weighted (2500/15-90/1) sequences, the former was repeated after intravenous administration of 0.1 mmol/kg Gd-DOTA. Slice thickness varied from 4 to 7 mm depending on the extent of the lesion. The signal intensities on the unenhanced images were compared to brain tissue: less intense(–), isointense(0) or more intense(+). En-

Table 1. Clinical and pathological data

Case	Age Sex	Bones involved	Presentation	Pathological examination Cellularity/calcification	Angiectasia/ sinusoids
1	15 F	Temporal bone and occipital, parietal, frontal and sphenoidal vault (P)	Dysequilibrium, deformity of skull vault, narrowing of external auditory canal, conductive hearing loss	0/0	Absent
2	57 F	Mandible (M)	Alveolar pain, prosthesis no longer fits	0/1	Few
3	13 F	Maxilla (M)	Deformaty left cheek	1/1	Few
4	37 F	Sphenoid bone, lumbar vertebra (P)	Visual impairment	1/1	Several
5	44 F	Orbital roof-frontal bone (M)	Small supraorbital lump	0/0	Several

(M), Monostotic form; (P), polyostotic form

Table 2. Clinical and pathological activity

Case	Clinical activity Pain or cranial nerve involvement[a]/Deformity[b]	Pathological activity Cellularity[c]/Calcification[d]	Combined activity
1	1/1	0/0	2
2	1/1	0/1	3
3	0/1	1/1	3
4	1/0	1/1	3
5	0/0	0/0	0

[a] 0, No pain, no palsies; 1, pain and/or palsies
[b] 0, No deformities; 1, skull or facial deformity
[c] 0, Moderate; 1, pronounced
[d] 0, More than 50%; 1, less than 50% calcification

Table 3. MRI findings and correlation with clinical/histological activity

Case	T1-weighted signal intensity	T2-weighted signal intensity	Gadolinium enhancement	Combined clinical and histological activity
1	Low	Low, isointense	Moderate	2
2	Low, high	Isointense, high	Marked	3
3	Low, high	Low, high	Moderate	3
4	Isointense, high	Isointense, high	Marked	3
5	Low, isointense	Low	Moderate	0

hancement was assessed as moderate (less intense than fat = +) or marked (isointense with or more intense than fat = + +). Activity of the lesions was quantified clinically: cranial nerve palsies or pain and growth or extension of the craniofacial lesions were considered to indicate activity [10, 11]; a score of 0 or 1 was allotted to each. In the same way the histological activity was graded by the amount of calcification (bone islands and woven bone) in the lesions (< 50% = 1, > 50% = 0) and by the degree of cellularity of the uncalcified parts of the lesions [5]; moderate cellularity with more pronounced sclerosis (score 0) or vice versa (score 1) can be found. This scoring system was further used to allow comparison between MRI findings and the clinical and pathological activity of the lesions. Finally, the pathologist paid special attention to the presence of enlarged veins, sinusoids and abnormal arteries, a possible explanation for gadolinium enhancement.

Results

Clinical and pathological data are presented in Table 1. In two patients (cases 1,2) both pain or nerve involvement and bone deformities were found on clinical examination; in one (case 4) cranial nerve involvement only was detected and in one only deformity of the facial skeleton. High cellularity and few islands of calcification were found by the pathologist in cases 3 and 4, while in case 1 only moderate cellularity was found, but calcification of the lesion was limited. Clinical and histological scoring showed three lesions to be active, one moderately active and one inactive (Table 2).

The MRI findings are listed in Table 3. In cases 2–4 small regions of high signal intensity on T1-weighted and T2-weighted images were seen. Marked enhancement with gadolinium was seen in two of these (cases 2 and 4). Marked differences in signal intensity within a lesion were seen on T1-weighted images in four cases and on T2-weighted images in three. In case 4 most of the lesion gave intermediate signal on T1-weighted images and marked enhancement was seen after gadolinium. In three patients only moderate enhancement was seen after gadolinium administration. In only one case were no dilated veins or large sinusoids detected. In all cases no abnormal arteries were found.

Discussion

FD most often affects and young adults adolescents. The disease is monostotic in 70% of cases [11], involvement of the ribs and femurs being most frequent. Cranio facial lesions are more frequent (40–60%) in the polyostotic than in the monostotic (25%) form and are usually unilateral. The clinical diagnosis can be confirmed with plain radiography, bone scintigraphy [12] or CT. FD is also often found in incidentally, but pathological confirmation is sometimes needed to confirm the diagnosis [8]. However, pathological differentiation from aneurysmal bone cyst (in case 3) and osteoblastoma (in case 2) was difficult, and a second, more representative biopsy was needed to make the final diagnosis. The MRI picture of FD has been described [11–13]. Initial studies reported low signal on T1- and T2-weighted spin-echo images [14], as seen throughout the lesion in cases 1 (Fig. 1) and 5 and in large parts of the affected bone in case 3. Fibrous tissue is responsible for this low to intermediate signal intensity [13]. Varying signal intensity, including higher intensity on T2-weighted images, has been explained by the complex histology of FD, and because the lesion is metabolically active [12]. A lesion of mainly high signal intensity on T2-weighted images was seen in case 2. In cases 3 and 4 only small regions showed high signal intensity on T2-weighted images, which were of intermediate (case 3; Fig. 2) or high (case 4; Fig. 3) intensity on T1-weighting and probably represent cyst formation and bleeding into the cyst [8]. Most of these signal patterns have been described in patients with FD of the long bones of the limbs [8, 12]. Only a few reports have dealt with gadolinium enhancement in FD, and the most extensive concerning the long bones [8]. We found enhancement in all our cases and in two a large part (case 2) or nearly all the lesion (case 4; Fig. 3) became as intense as or more intense than fat. These two patients had lesions active both clinically and histologically (Table 2). In case 4 deformity of the sphenoid was marked, but due to its deep location it was not detected clinically, resulting in an underestimation of activity. Both strongly enhancing lesions had regions of high intensity on both T1- and T2-weighted images (Fig. 3). Unfortunately, marked enhancement with gadolinium is not always present in clinically and pathologically active lesions or in lesions with high signal intensity regions on both spin-echo sequences (Fig. 2). However, in all three patients with the highest combined "clinical-pathological" activity (cases 2–4) high-intensity regions were seen on both spin-echo sequences. The reason for the enhancement in fibrous dysplasia is unknown. Probably the fibrocellular tissue replacing the normal bone marrow is responsible for the enhancement. Enhancement is seen in fibrous lesions with low signal intensity on both sequences (Figs. 1, 4). Why more marked enhancement was present in two of the three

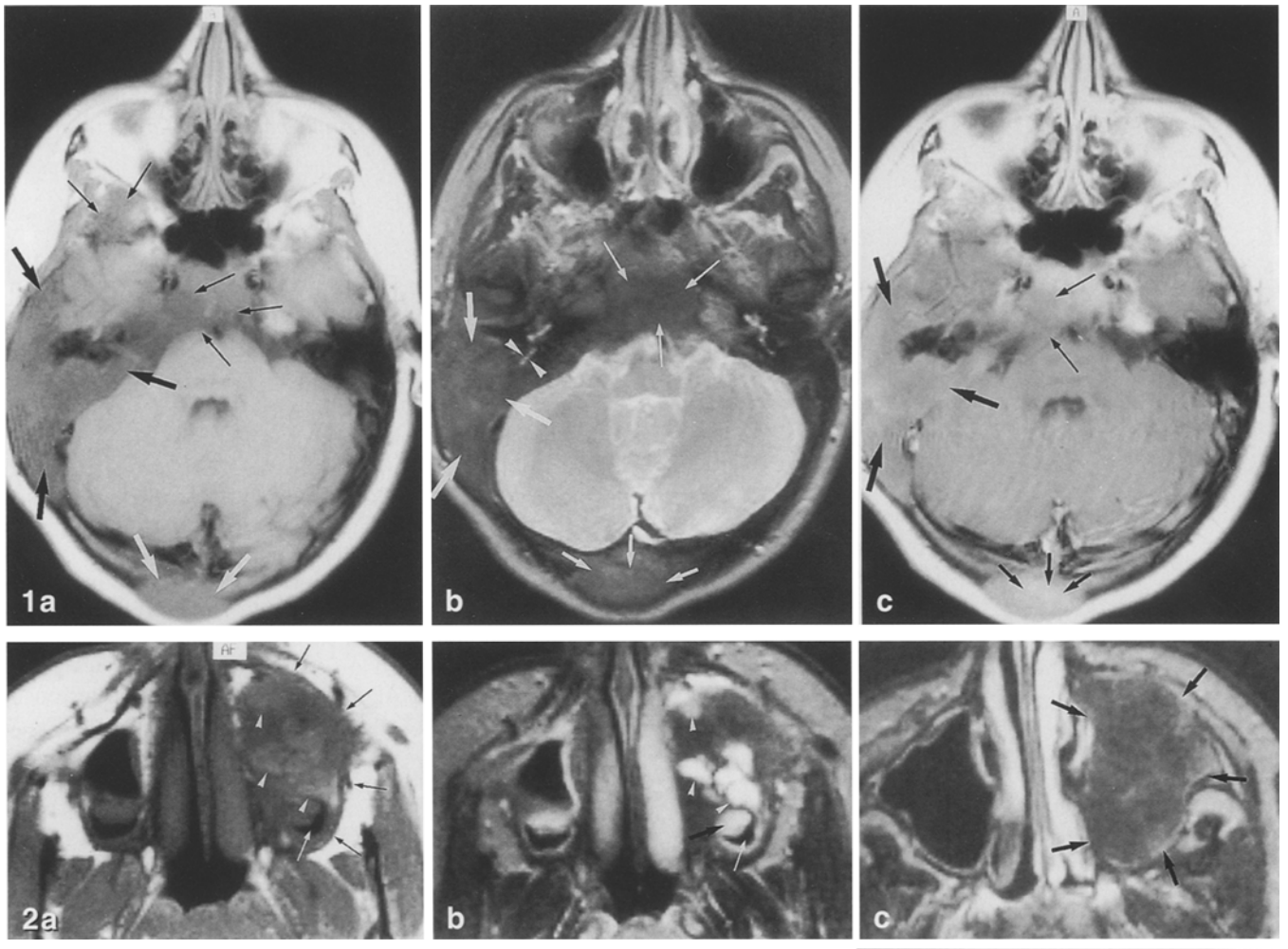

Fig. 1a–c. Fibrous dysplasia of temporal bone and skull vault (case 1). Axial images taken at the level of the inner ear. Low intensity on T1-, low to intermediate intensity on T2-weighted images; moderate enhancement.
a T1-weighted image (600/15/2) shows bone thickening and signal change in occipital *(large white arrows)*, sphenoid *(long black arrows)* and temporal *(large black arrows)* bone. The intensity is homogeneous and lower than that of brain.
b T2-weighted image (2500/90/1). The signal in the occipital *(small white arrows)*, sphenoid *(long white arrows)* and temporal *(large white arrows)* lesions remains lower than that of brain. Notice the high intensity of the endolymph in the right posterior semicircular canal *(white arrowheads)* surrounded by abnormal bone.
c Gd-enhanced T1-weighted image (600/15/2). Moderate homogeneous enhancement is seen in the occipital *(small black arrows)*, sphenoid *(long white arrows)* and temporal *(large black arrows)* lesions, but their intensity remains lower than that of the subcutaneous fat

Fig. 2a–d. Fibrous dysplasia of the left maxilla (case 3). Low signal intensity on T1-weighted and foci of high intensity on T2-weighted images; moderate contrast enhancement. **a** Axial T1-weighted image (600/15/2). Involvement of the left maxilla with convex protrusion of the anterior and lateral walls of the sinus towards the surrounding soft tissues *(long black arrows)*. The lesion was hypointense compared to brain although some slightly hyperintense regions were noted *(white arrowheads)*. Air is present only posteriorly in the maxillary sinus *(long white arrow)*. **b** T2-weighted image (2500/90/1) at same level. The regions of intermediate signal become of high intensity *(white arrowheads)*. A low intensity region on the T1-weighted image is of high intensity on T2-weighting *(large black arrow)*, this probably corresponds to a proton-rich part of the lesion, which is not purely cystic (see **d**). Air is again seen *(long white arrow)*. **c** T2-weighted image (2500/90/1) 1 cm more craniad. Most of the lesion remains hypointense, filling the enlarged maxillary sinus *(large black arrows)*. **d** Gd-enhanced image at same level as **a**. All the lesion has increased slightly in intensity but more marked enhancement is seen at the borders of the intermediate intensity regions on the T1-weighted image *(white arrowheads)* and the most marked enhancement was seen in a more posterior, proton-rich part of the lesion *(small white arrows)*

clinically and pathologically active cases, with high signal intensity on both T1- and T2-weighted images (cases 2–4) is still unknown. FD lesions are well vascularized [10, 12] and angiectasia or large peripheral sinusoids can be present. In our study no histological explanation was found for the marked enhancement and as angiectasia or sinusoids were present not only in the two markedly enhancing lesions but also in two which enhanced only moderately, this feature fails to explain the difference in enhancement pattern. The cellularity of the lesions did not correlate well with the enhancement pattern [1]. A possible explanation is that biopsies are often too small and not truly representative of the total lesion.

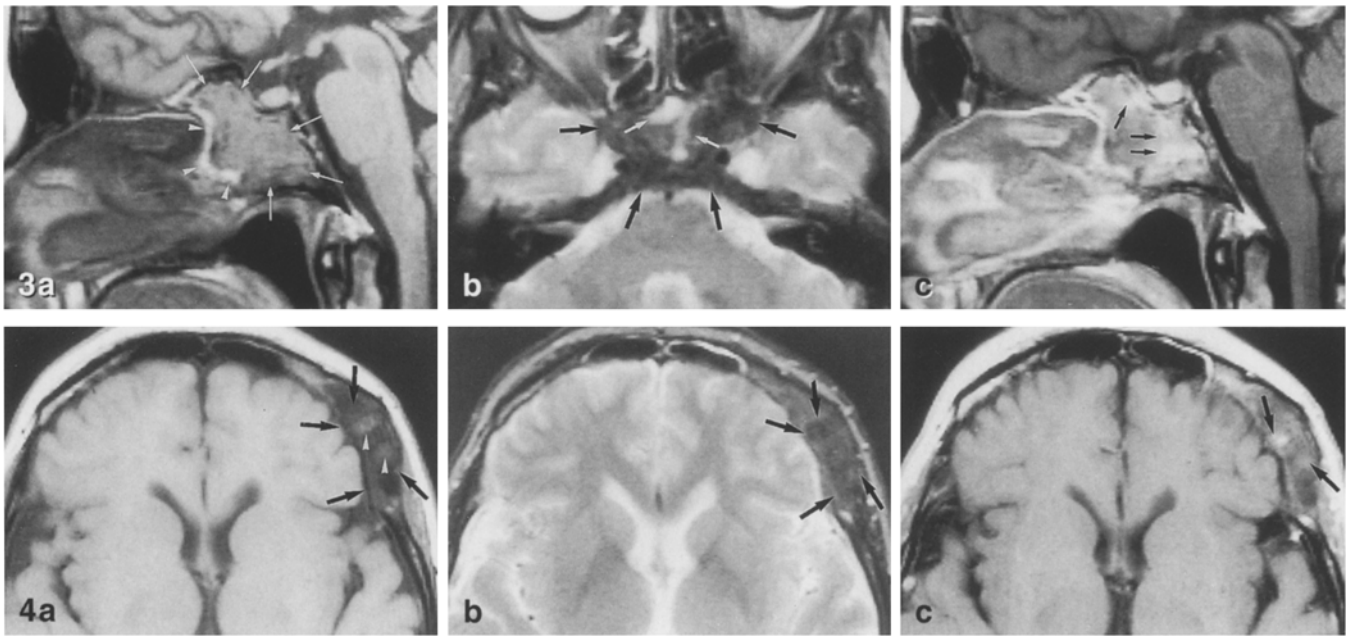

Fig. 3 a–c. Fibrous dysplasia of the sphenoid bone with obliteration of the sinus (case 4). Intermediate signal intensity on T1- and T2-weighted images (with small region of high intensity on both); marked contrast enhancement. **a** Sagittal T1-weighted image (600/15/2). The abnormal bone of the sphenoid sinus *(long white arrows)* is isointense with brain tissue and a small rim of high intensity is seen anteroinferiorly *(white arrowheads)*. **b** Axial T2-weighted image (2500/90/1) through the inferior border of the lesion. Low intensity is seen in most of the sphenoid sinus *(large black arrows)*. The anteroinferior border of the lesion remains of high intensity *(small white arrows)* and probably represents cyst formation or bleeding. **c** Sagittal Gd-enhanced T1-weighted image (600/15/2). Inhomogeneous enhancement is seen throughout the sphenoid sinus and marked enhancement (as bright or even brighter than fat) is seen in the posterosuperior part of the lesion *(small black arrows)*

Fig. 4 a–c. Fibrous dysplasia of the left orbital roof and frontal bone (case 5). Low signal intensity on T1- and T2-weighted images; moderate contrast enhancement. **a** Axial T1-weighted image (600/15/2). Enlargement of the frontal bone *(large black arrows)*; most of the lesion is of low intensity, although two small isointense spots *(white arrowheads)* are visible. **b** Axial T2-weighted image (2500/90/1) at the same level. The lesion *(large black arrows)* remains hypointense. **c** Axial Gd-enhanced T1-weighted image. Enhancement is seen throughout the lesion; the signal intensity approaches that of fat in the two small spots which were of relatively high signal intensity on the unenhanced image *(large black arrows)*

References

1. Kransdorf MJ, Moser RP, Gilkey FW (1990) From the archives of the AFIP. Fibrous dysplasia. Radio Graphics 10: 519–537
2. Som PM (1991) Sinonasal cavity. In: Som PM, Bergeron RT (eds) Head and neck imaging 2nd edn. Mosby, St. Louis, pp 51–276
3. Leeds N, Seaman WB (1962) Fibrous dysplasia of the skull and its differential diagnosis. A clinical and roentgenographic study of 46 cases. Radiology 78: 570–582
4. Daffner RH, Kirks DR, Gehweiler JA, et al (1982) Computed tomography of fibrous dysplasia. AJR 139: 943–948
5. Eich GF, Babyn P, Armstrong D, Burrows P, Posnick JC, Becker L (1990) An unusual case of craniofacial fibrous dysplasia presenting in early infancy. Pediatr Radiol 20: 495–498
6. Wackerle B, Reiser M, Herzog M, Kahn T (1987) Radiologische Befunde bei Cherubismus – Orthopantomographie, CT and MR. Röntgenpraxis 40: 104–107
7. Wilbur AC, Dobben GD, Linder B (1987) Paraorbital tumors and tumorlike conditions: role of CT and MRI. Radiol Clin North Am 25: 631–646
8. Stiglbauer R, Ritschl P, Kramer J, Imhof H (1989) Fibrose Dysplasie: Erscheinungsbild im Magnetresonanztomogramm. Fortschr Röntgenstr 151: 338–341
9. Curtin HD, Hirsch WL (1991) Base of the skull. In: Atlas SW (ed) Magnetic resonance imaging of the brain and spine. Raven Press, New York, pp 669–708
10. Ito H, Waga S, Sakakura M (1985) Fibrous dysplasia of the skull with increased vascularity in the angiogram. Surg Neurol 23: 408–410
11. Brette MD, Wassef M, Le Guillou C, Hadjean E, Tran Ba Huy P (1987) Dysplasie fibreuse et fibrome ossifiant de la base du crane, à propose de 6 cas. Ann Otolaryngol (Paris) 104: 441–453
12. Utz JA, Kransdorf MJ, Jelinek JS, Moser RP, Berrey BH (1989) MR appearance of fibrous dysplasia. J Comput Assist Tomogr 13: 845–851
13. De Schepper AM, Degryse HR (1988) Fibrous dysplasia. In: De Schepper AM, Degryse HR (eds) Magnetic resonance imaging of bone and soft tissue tumors and their mimics. Kluwer, Dordrecht, pp 61–68
14. Harms SE, Greenway G (1988) Musculoskeletal system. In: Stark DD, Bradley WG (eds) Magnetic resonance imaging: Mosby, St. Louis, pp 1323–1433

Dr. J. W. Casselman
Department of Radiology
A. Z. St.-Jan Bruges
Ruddershove 10
B-8000 Bruges, Belgium